Geochemical proxies of North American freshwater routing during the Younger Dryas Cold Event

Anders E. Carlson[1]*†, Peter U. Clark[1], Brian A. Haley[2], Gary P. Klinkhammer[3], Kathleen Simmons[4], Edward J. Brook[1], Katrin J. Meissner[5]

[1]*Department of Geosciences, Oregon State University, Corvallis, OR 97331, USA*

[2]*IfM-GEOMAR, 24148 Kiel, Germany*

[3]*College of Oceanic and Atmospheric Sciences, Oregon State University, Corvallis, OR 97331, USA*

[4]*U.S. Geological Survey, Denver, CO 80225, USA*

[5]*School of Earth and Ocean Sciences, University of Victoria, Victoria, BC, V8W 3P6, Canada*

*To whom correspondence should be addressed.

E-mail: acarlson@whoi.edu, Phone: 508-289-3976, Fax: 508-457-5187

† Present address: *Department of Geology and Geophysics, Woods Hole Oceanographic Institution, Woods Hole, MA 02543, USA*

Major Category: Physical Sciences

Minor Category: Geology

Text Pages: 20

Supporting Online Methods Pages: 9

Figures: 5

Supporting Online Figures: 1

Tables: 1

Supporting Online Tables: 1

Abstract Word Count: 230

Total Character Count: ~33,600

Abbreviations: Sverdrup: Sv; Atlantic meridional overturning circulation: AMOC; calibrated years before present: cal. yr BP; sea surface temperature: SST; kiloyears before present: kyr BP; practical salinity units: psu.

The Younger Dryas cold interval represents a time when much of the Northern Hemisphere cooled from ~12.9 to 11.5 kiloyears before present. The cause of this event, which has long been viewed as the canonical example of abrupt climate change, was initially attributed to the routing of freshwater to the St. Lawrence River with an attendant reduction in Atlantic meridional overturning circulation. However, this mechanism has recently been questioned because current proxies and dating techniques have been unable to confirm that eastward routing with an increase in freshwater flux occurred during the Younger Dryas. Here we use new geochemical proxies (ΔMg/Ca, U/Ca & $^{87}Sr/^{86}Sr$) measured in planktonic foraminifera at the mouth of the St. Lawrence Estuary as tracers of freshwater sources to further evaluate this question. Our proxies, combined with planktonic $\delta^{18}O_{seawater}$ and $\delta^{13}C$, confirm that routing of runoff from western Canada to the St. Lawrence River occurred at the start of the Younger Dryas, with an attendant increase in freshwater flux of 0.06 ± 0.02 Sverdrup (1 Sverdrup (Sv) = 10^6 m^3 s^{-1}). This base discharge increase is sufficient to have reduced Atlantic meridional overturning circulation and caused the Younger Dryas cold interval. In addition, our data indicate subsequent fluctuations in the freshwater flux to the St. Lawrence River of ~0.06 to 0.12 Sv, thus explaining the variability in the overturning circulation and climate during the Younger Dryas.

Proxies of deepwater formation show that a large reduction in the Atlantic meridional overturning circulation (AMOC) occurred at the start of the Younger Dryas event (1-3), suggesting that the attendant loss of ocean heat transport caused Younger Dryas cooling in the North Atlantic region. The cause of this ocean response remains unclear, however, with the leading mechanism, involving the routing of continental runoff to the St. Lawrence River (4-8), now questioned on the basis of marine (9-11) and terrestrial (12, 13) evidence, and modeling (14). Moreover, the rate of the AMOC varied during the Younger Dryas (1-3), which is not readily explained by the conventional routing argument (4-8). This debate has led to the questioning of the role of freshwater in forcing abrupt climate change (13), with important implications to our understanding of the sensitivity of the AMOC to global warming and attendant changes in the hydrological cycle.

Here we capitalize on the well-known relation between river geochemistry and underlying bedrock lithology (15) to use changes in $^{87}Sr/^{86}Sr$, U/Ca, and Mg/Ca measured in planktonic foraminifera tests as tracers of routing of continental runoff derived from distinct geological terranes. The conventional argument for the cause of the Younger Dryas (4-8) invokes the opening of the eastern Lake Agassiz outlet and the Straits of Mackinaw ~12,900 calibrated years before present (cal. yr BP) (all dates reported here are in calibrated radiocarbon years unless otherwise specified) by retreat of the southern Laurentide Ice Sheet margin, effectively doubling the size of the St. Lawrence River drainage basin, from 1.35×10^6 km^2 to 3.13×10^6 km^2 (7) (Fig. 1). Because the newly added drainage area included significantly different bedrock lithologies than those underlying the St. Lawrence drainage area prior to this event (16) (Fig. 1), the associated routing of surface water should thus be marked by changes in St. Lawrence water geochemistry (15). In order to assess geochemical changes associated with

these new sources of surface water, we picked planktonic foraminifera from two cores in the outer St. Lawrence estuary (Fig. 1) that span the Younger Dryas interval: *G. bulloides* and *N. pachyderma (s)* from core HU90031-047 (45°51.14'N, 57°37.56'W; 473 m depth), and *G. bulloides* from core HU90031-044 (44º39.41'N, 55º37.13'W; 1381 m depth).

Results

Changes in Mg/Ca, U/Ca and $^{87}Sr/^{86}Sr$ identify changes in the source and flux of surface waters reaching the St. Lawrence estuary during the Younger Dryas (Fig. 2). Mean Mg/Ca values in *G. bulloides* from core 044 range from 1.1 to 3 mmol/mol (Fig. 2d). Changes in Mg/Ca in foraminifera reflect temperature- and salinity-dependent uptake of Mg as well as changes in the [Mg] and [Ca] of the water (17, 18). We use an existing sea surface temperature (SST) record from core 044, based on dinoflagellate-cyst assemblages (11) (Fig. 2a), to account for SST changes in our Mg/Ca record by applying the *G. bulloides* calibration (Mg/Ca (mmol/mol) = 0.474exp[0.107 x SST(^{o}C)]) (18). The persistence of sea ice in the St. Lawrence estuary for 9 months out the year during the Younger Dryas (11) indicates that planktonic foraminifera grew in the 3 months of summer, the season of the SST reconstruction. We then estimate salinity variations in the estuary on the basis of a $\delta^{18}O_{seawater}$ record from core 044 (Fig. 2b), and applied a salinity calibration (Mg/Ca (mmol/mol) = 0.311 x salinity) (18). These combined corrections have a propagated error of ~30% (16) (see supporting online methods). Subtracting these temperature and salinity components from our measured Mg/Ca values and normalizing to the lowest resulting value produces a ΔMg/Ca record that reflects changes in Mg/Ca of the estuary.

Foraminiferal ΔMg/Ca increases by ~2.5 mmol/mol at the onset of the Younger Dryas (Fig. 2d), a signal that had been masked in our Mg/Ca record by the corresponding decrease in SST and salinity (Fig. 2a, 2b). We attribute this increase to the routing of western Canadian

runoff to the St. Lawrence River due to retreat of ice out of the Lake Superior Basin. Specifically, rivers draining shale and carbonate bedrock in areas of western Canadian Plains that were routed to the St. Lawrence basin during the Younger Dryas (Fig. 1) have [Mg] that are ~6 to 10 times higher (~0.6 to 1.0 mmol/kg) than the [Mg] of the integrated St. Lawrence River system (~0.1 mmol/kg) (19) prior to the Younger Dryas. At ~12.7 kiloyears before present (kyr BP), ΔMg/Ca increases again by ~1.5 mmol/mol, indicating a further increase in freshwater flux from western Canadian Plains.

Using our geochemical mixing model and assuming similar river chemistry as today and a pre-Younger Dryas flux of 0.07 Sverdrup (7) (1 Sverdrup (Sv) = 10^6 m^3 s^{-1}), we find that an increase of 0.07 Sv in freshwater discharge for the St. Lawrence River (Fig. 3) derived from these source waters would explain the initial Younger Dryas ΔMg/Ca signal (see supporting online methods). The subsequent increase in ΔMg/Ca at 12.7 kyr BP can be explained by an additional flux increase of 0.06 Sv (Fig. 3). Because the dinoflagellate-cyst SST reconstruction records temperature near the water surface whereas *G. bulloides* may live deeper in the mixed layer, the increases in ΔMg/Ca and modeled base flow discharge during the Younger Dryas are maximum estimates. However, evidence for atmospheric cooling in Maritime Canada (20) and mixed-layer cooling in the shelf water of the North Atlantic adjacent to the St. Lawrence estuary (10) provides strong support for substantial cooling of the St. Lawrence estuary during the Younger Dryas and the temperature correction.

Foraminiferal U/Ca in *G. bulloides* and *N. pachyderma (s)* from core 047 and in *G. bulloides* from core 044 all reach peak values that are ~30 to 35 nmol/mol higher in Younger Dryas samples relative to older samples (Fig. 2e). The primary sources of seawater U are from U dissolved in rivers, by colloid and particulate disintegration at high salinities (practical salinity

units (psu) >20) (21), and by release from marine sediments in response to an increase in bottom-water oxygen, such as may be associated with an increased flux of oxygenated freshwater into the St. Lawrence estuary during a routing event. Assuming reasonable values for [U] (25 ppm) in sediment with a 1-meter sediment mixed-layer depth distributed over the area of the estuary, a change from anoxic to oxic conditions would release 24 x 10^6 moles of U to the estuary, corresponding to a foraminiferal U/Ca signal of ~0.7 nmol/mol (22), or significantly less than our measured values. On the other hand, rivers draining shale and carbonate bedrock of the western Canadian Plains (Fig. 1) have average [U] (10 to 20 nmol/kg) that are 10 to 20 times greater than the [U] of the integrated St. Lawrence River system (23) prior to the Younger Dryas. Our measured increase in U/Ca is thus consistent with the routing of U-rich surface waters from the western Canadian Plains following the opening of the eastern outlet of Lake Agassiz.

Unlike the ΔMg/Ca record, however, the initial U/Ca increase is gradual until 12.7 kyr BP when it rapidly rises to a peak at 12.5 kyr BP. We attribute the slow initial rise in U/Ca to the offsetting effect of [CO_3^{-2}] on U/Ca in foraminifera tests, such that a doubling to tripling of [CO_3^{-2}] discharged into the estuary due to the increased area draining carbonate terranes would reduce the U/Ca in foraminifera tests by ~4 nmol/mol (24). Moreover, U release from colloid and particulate disintegration at high salinities will increase exponentially with river flux (see supporting online methods). By including the carbonate ion effect and the break-down of colloids and particulates, our mixing model of estuary geochemistry indicates that an increase in discharge through the St. Lawrence River of 0.05 Sv at the start of the Younger Dryas would explain the ~10 nmol/mol increase in foraminiferal U/Ca, with an additional flux increase of 0.05 Sv at 12.7 kyr BP explaining the subsequent peak U/Ca values (Fig. 3) (see supporting online methods).

Foraminiferal $^{87}Sr/^{86}Sr$ show little change at the start of the Younger Dryas, followed by a rapid increase in $^{87}Sr/^{86}Sr$ at 12.5 kyr BP that is 7 x 10^{-5} higher than $^{87}Sr/^{86}Sr$ in samples that predate the Younger Dryas (Fig. 2f). Global seawater $^{87}Sr/^{86}Sr$ is invariant on this timescale, whereas river $^{87}Sr/^{86}Sr$ varies as a function of bedrock age and the duration of chemical weathering of granitoid sediment (25), suggesting that these fluctuations reflect changes in the $^{87}Sr/^{86}Sr$ and flux of runoff to the St. Lawrence River. At the time of initial opening of the eastern Lake Agassiz outlet, exposed western Canadian Precambrian Shield had been deglaciated for at least 1,000 years (26), so that $^{87}Sr/^{86}Sr$ of granitoid sediment would be comparable to modern bedrock values (0.72450) (25). Our mixing model (see supporting online methods) indicates that an initial flux increase of 0.06 Sv at the start of the Younger Dryas (Fig. 3) (as suggested by ΔMg/Ca and U/Ca) with higher $^{87}Sr/^{86}Sr$ associated with older bedrock of the western Canadian Shield than the younger bedrock of the eastern Canadian Shield (0.71423) (27) would cause foraminiferal $^{87}Sr/^{86}Sr$ to increase by 1 x 10^{-5}, which is within the uncertainty of our measurements in the early Younger Dryas samples. Subsequent retreat of the southwestern LIS margin (26) (Fig. 1), which was likely enhanced by atmospheric feedbacks associated with the enlarging area of Lake Agassiz (28), exposed Precambrian Shield bedrock, thus spiking runoff with high $^{87}Sr/^{86}Sr$ (0.79500) due to the release of radiogenic Sr from young granitoid soils (25). Assuming initial $^{87}Sr/^{86}Sr$ similar to modern values in surface waters of Canada (27), we find that a subsequent increase in freshwater flux of 0.06 Sv (Fig. 3) combined with radiogenic Sr derived from weathering of freshly exposed granitoid sediment following ice retreat explains the abrupt increase in $^{87}Sr/^{86}Sr$ at 12.5 kyr BP (see supporting online methods).

Discussion

Our multiproxy approach addresses the fact that, for any given proxy, additional factors

(i.e., temperature, weathering) modulate the signal of changes in freshwater flux. In doing so, we find a clear signal of routing of surface waters from western Canada to the St. Lawrence River at the start of the Younger Dryas, as originally proposed by Johnson and McClure (4). In particular, our three geochemical tracers of source waters independently converge in indicating that freshwater discharge through the St. Lawrence River increased by 0.06 ± 0.02 Sv (average of our three estimates with 2 sigma error) at the start of the Younger Dryas with a subsequent increase of 0.06 ± 0.01 Sv during the Younger Dryas for a total flux increase of 0.12 ± 0.02 Sv. Our estimate of the initial flux increase (0.06 ± 0.02 Sv) is in good agreement with a previously estimated flux of ~0.07 Sv (7). The total freshwater flux increase of 0.12 ± 0.02 Sv would decrease estuarine mixed-layer salinity by 4.1 ± 0.6 psu.

The planktonic $\delta^{13}C$ record in core 044 provides additional support for substantial changes in freshwater flux to the Gulf of St. Lawrence during the Younger Dryas. The $\delta^{13}C$ of dissolved inorganic carbon in freshwater primarily reflects some combination of the $\delta^{13}C$ of soil CO_2 derived from decay of organic matter (lighter values) and the $\delta^{13}C$ of any underlying carbonate bedrock (heavier values). We attribute the abrupt 0.32 per mil decrease in $\delta^{13}C$ (the only anomaly in the 14.5-kiloyear record; reproducibility <0.05 per mil) at the start of the Younger Dryas (Fig. 2c) to indicate an increased flux of ^{12}C-enriched surface runoff reflecting the routing of freshwater from the western Canadian Plains to the St. Lawrence. However, $\delta^{13}C$ does not show any change at a time (12.7 to 12.5 kyr BP) when ΔMg/Ca, U/Ca and $^{87}Sr/^{86}Sr$ suggest an increase in freshwater flux. This lack of a signal may reflect a larger contribution from ^{12}C-depleted bedrock relative to soil CO_2, thus offsetting any change in $\delta^{13}C$ associated with an increased freshwater flux.

These combined results appear contrary to the modest 0.5 per mil decrease in $\delta^{18}O_{calcite}$ measured in *N. pachyderma (s)* from core 044 (Fig. 2b), which deVernal *et al.* (11) used along with salinity reconstructions based on dinoflagellate-cysts to argue against any significant salinity decrease in the St. Lawrence estuary during the Younger Dryas. However, $\delta^{18}O_{calcite}$ reflects the combination of the offsetting effects of temperature and salinity, so that a 10°C decrease in SSTs during the Younger Dryas at this site (11) (Fig. 2a) would mask an additional 2.25 per mil salinity signal in $\delta^{18}O_{calcite}$, corresponding to a net 2.75 per mil decrease in $\delta^{18}O_{seawater}$ (Fig. 2b). Similar to the ΔMg/Ca record, this total 2.75 per mil $\delta^{18}O_{seawater}$ decrease is a maximum estimate due to the depth-habitat difference between the dinoflagellates (the SST source) and *N. pachyderma (s)*. However, a freshwater flux increase of 0.11 Sv (Fig. 3) derived from western Canadian source waters with $\delta^{18}O$ of -25 per mil (29) would have decreased estuarine mixed-layer $\delta^{18}O$ by 2.75 per mil (see supporting online methods). This flux increase is in good agreement with the estimated increase (0.12 ± 0.02 Sv) from our three routing proxies, thus supporting the temperature correction in core 044.

We note that the stacked $\delta^{18}O_{calcite}$ record measured on *N. pachyderma (s)* from the continental margin off Nova Scotia also shows a ~0.8 per mil decrease during the Younger Dryas (10) (supplementary online Fig. 6a & b), which, if corrected for Younger Dryas cooling suggested by the large increase in % *N. pachyderma (s)* from the same cores (supporting online Fig. 6c), would approach the $\delta^{18}O_{seawater}$ change suggested from St. Lawrence estuary (see supporting online methods and Fig. 6b). In addition, open ocean $\delta^{18}O_{calcite}$ records measured on *G. bulloides* and *N. pachyderma (s)* from Orphan Knoll show a 1 to 1.25 per mil decrease during the Younger Dryas (30), which would be closer to the $\delta^{18}O_{seawater}$ change in the St. Lawrence estuary if the temperature decrease was taken into account. The salinity decrease in the St.

Lawrence is also contemporaneous with a 2.5 to 2.75 per mil increase in $\delta^{18}O_{seawater}$ from the Orca Basin, Gulf of Mexico (31) (Fig. 2b), thus supporting Johnson and McClure's hypothesis (4) that routing of North American runoff from the Mississippi to the St. Lawrence River occurred at the start of the Younger Dryas. While the dinoflagellate-cyst salinity reconstruction of de Vernal *et al.* (11) lacks a freshening signal, the combined evidence from our $^{87}Sr/^{86}Sr$, U/Ca, and ΔMg/Ca records as well as the planktonic $\delta^{13}C$ and $\delta^{18}O_{seawater}$ records all indicating reduced salinity suggest that the dinoflagellate-cyst salinity reconstruction for the St. Lawrence estuary is in error during the Younger Dryas.

According to the conventional routing hypothesis, surface waters from western Canada continued to drain through the eastern outlet of Lake Agassiz to the St. Lawrence River until ~11.5 kyr BP, when ice readvance across the outlet rerouted surface waters either to the south (Mississippi River) (6-8) or to the northwest (Mackenzie River) (32) (Fig. 1). In contrast, all proxies from core 044 indicate that salinity started to increase ~12.3-12.4 kyr BP, and reached pre-Younger Dryas values by ~12 kyr BP (Fig. 2) implying a decrease to pre-Younger Dryas freshwater discharge (Fig. 3) and suggesting that rerouting occurred earlier. The terrestrial record of routing during this time period is poorly constrained, but two lines of evidence suggest that this previously unrecognized intra-Younger Dryas routing event occurred through the northwestern Clearwater Outlet to the Arctic Ocean via the Mackenzie River (Fig. 1): a radiocarbon age of 10,310 $\pm$ 290 ^{14}C yr BP (12,040 $\pm$ 400 cal. yr BP) on a piece of wood obtained in flood deposits from the outlet (32) with two additional supporting radiocarbon dates on wood of the same age (33), and a light planktonic $\delta^{18}O$ anomaly in a record from the Beaufort Sea that dates at 12 kyr BP (34) using the most recent reservoir age for this region (26).

Three proxies from core 044 (U/Ca, $^{87}Sr/^{86}Sr$ and $\delta^{13}C$) indicate that freshwater flux to the St. Lawrence River subsequently increased for the remainder of the Younger Dryas, whereas $\delta^{18}O_{seawater}$ and ΔMg/Ca show no change (Fig. 2). We attribute the increase in $^{87}Sr/^{86}Sr$, U/Ca and $\delta^{13}C$ to renewed routing of western Canadian runoff to the St. Lawrence, possibly due to isostatic uplift of the northwest outlet to the Arctic Ocean, causing Lake Agassiz waters to again start draining to the east. Based on our geochemical modeling, this subsequent rerouting would have increased the flux out the St. Lawrence River by 0.06 $\pm$ 0.01 Sv (Fig. 3) (see supporting online methods). The absence of an equivalent ΔMg/Ca signal at this time may in part reflect source-rock changes in the eastern Great Lakes region, whereby the opening of more northerly outlets allowed westerly-derived waters from the Agassiz basin to bypass Lakes Erie and Ontario and flow directly from Lake Huron into the St. Lawrence River by way of the Ottawa River (9, 26). The attendant loss of Mg-rich waters due to bypassing the dolomites of the Erie and Ontario basins (Fig. 1) would thus have counteracted the gain of Mg-rich waters derived from the Agassiz basin. However, we should expect to see a ~2.5 to 4 mmol/mol gain in ΔMg/Ca relative to a loss of ~1 mmol/mol due to bypassing carbonate bedrock of the eastern Great Lakes. The absence of a ΔMg/Ca signal as well as a $\delta^{18}O_{seawater}$ signal during this late Younger Dryas time may thus result from the ~30% error in the ΔMg/Ca record (see supporting online methods) due to the temperature and salinity adjustments (18) and the ~20% error in the SST reconstruction (11) with its propagated effect on $\delta^{18}O_{seawater}$.

Our source-water tracers thus provide the first direct oceanographic evidence of eastward routing of surface waters from western Canada to the St. Lawrence River at the start of the Younger Dryas. According to climate models, our estimated freshwater flux increase (0.06 ± 0.02 Sv initially, 0.12 ± 0.02 Sv maximum) required to produce measured changes in $^{87}Sr/^{86}Sr$,

U/Ca, ΔMg/Ca, and $\delta^{18}O_{seawater}$ would be sufficient to induce a significant reduction in the AMOC (35), such as occurred during the Younger Dryas (1-3) (Fig. 4). Our results thus resolve the timing of continental routing during this critical period of deglaciation and suggest that the increase in base flow discharge in the St. Lawrence River forced the Younger Dryas cold event. Our results also offer new strategies for investigating whether similar mechanisms may have been responsible for other abrupt climate changes.

In addition, our source-water tracers reveal the cause of ocean and climate variability that occurred during the Younger Dryas. All our routing proxies show that, rather than a constant flux of freshwater as generally implied by the conventional routing mechanism (7, 8), freshwater base discharge varied during the Younger Dryas with a two-stepped increase at the start of the Younger Dryas followed by a decrease to pre-Younger Dryas values centered at ~12 kyr BP when freshwater was diverted to the Arctic Ocean. This intra-Younger Dryas routing event is in excellent agreement with proxies that indicate an increase in the AMOC (1-3) (Fig. 4) and attendant warming of the surface ocean (36, 37) (Fig. 5d,f) and atmosphere (38-40) (Fig. 5a,b,c), increased southeast Asian monsoon intensity (41) (Fig. 5g), and a cooling over Antarctica (42) (Fig. 5h) during the Younger Dryas. These same proxies then suggest that the AMOC subsequently decreased (Fig. 4) with an attendant climate response at a time when our tracers suggest a rerouting of western Canadian freshwater back to the St. Lawrence River (Fig. 5). This tight coupling between changes in freshwater fluxes to the North Atlantic basin, changes in the AMOC, and changes in climate further emphasizes the sensitivity of the climate system to relatively small changes in the hydrological cycle.

Methods

Samples were physically cleaned, prepared with a flow-through method that removes any effects of diagenesis and overgrowths (43), and analyzed by high-resolution ICP-MS for U/Ca and Mg/Ca. Sr-isotopes were analyzed by multi-collector ICP-MS and TIMS. We constructed age models from previously published ^{14}C ages for 044 (11) and new ^{14}C dates from 044 and 047 (Table 1), giving us age control approximately every 430 years (Fig. 2). All ^{14}C ages are reservoir corrected (11, 26) and calibrated (44). The agreement between benthic mollusk shell ages and planktonic foraminifera ages (11) indicates that any changes in the freshwater flux to the estuary did not affect the reservoir age.

We thank A. deVernal and C. Hillaire-Marcel for isotope data; the Bedford Institute of Oceanography for samples; L. Keigwin for foraminifera count and isotope data; the Saskatchewan Watershed Authority for river chemistry data; A. Unger for assistance with flow-through processing; M. Cheseby and J. Padman for assistance with foraminifera picking; and D. Barber, G. Clarke, S. Hostetler, A. Mix, and D. Muhs for helpful comments and discussion. Comments and suggestions from two anonymous reviewers greatly improved this manuscript. This research was funded by the NSF Paleoclimate Program (P.U.C.) and the NSF (G.P.K.).

References

1. Hughen, K.A., Southon, J.R., Lehman, S.J. & Overpeck, J.T. (2000) *Science* **290**, 1951-1954 (2000).

2. McManus, J.F., Francois, R., Gherard, J.-M., Keigwin, L.D. & Brown-Leger, S. (2004) *Nature* **428**, 834-837.

3. Elgroth, S.F., Adkins, J.F., Robinson, L.F., Southon, J. & Kashgarian, M. (2006) *Paleoceanography* **21**, doi: 10.1029/2005PA001192.

4. Johnson, R.G. & McClure, B.T. (1976) *Quaternary Research* **6**, 325-353.

5. Rooth, C. (1982) *Progress in Oceanography* **11**, 131-149.

6. Broecker, W.S., Kennett, J.P., Flower, B.P., Teller, J.T., Trumbore, S., Bonani, G. & Wolffi, W. (1989) *Nature* **341**, 318-321.

7. Licciardi, J.M., Teller, J.T. & Clark, P.U. (1999) in *Mechanisms of Global Climate Change at Millennial Time Scales: Geophysical Monograph,* eds Clark, P.U., Webb, R.S., Keigwin, L.D. (AGU, Washington , D.C.) vol. 112, pp. 177-201.

8. Clark, P.U., Marshall, S.J., Clarke, G.K.C., Hostetler, S.W., Licciardi, J.M. & Teller, J.T. (2001) *Science* **293**, 283-287.

9. Rodrigues, C.G. & Vilks, G. (1994) *Quaternary Science Reviews* **13,** 923-944.

10. Keigwin, L.D. & Jones, G.A. (1995) *Paleoceanography,* **10,** 973-985.

11. deVernal, A., Hillaire-Marcel, C. & Bilodeau, G. (1996) *Nature* **381,** 774-777.

12. Teller, J.T. Boyd, M., Yang, Z., Kor, P.S.G. & Fard, A.M. (2005) *Quaternary Science Reviews* **24**, 1890-1905.

13. Lowell, T.V., Fisher, T.G., Comer, G.C., Hajdas, I., Waterson, N., Glover, K., Loope, H.M., Schaefer, J.M., Rinterknecht, V., Broecker, W. *et al.,* (2005) *EOS* **86**, 365-373.

14. Tarasov, L. & Peltier, W.R. (2005) *Nature* **435**, 662-665.

15. Meybeck, M. (1987) *American Journal of Science* **287,** 401-428.

16. Barton, K.E., Howell, D.G. & Vigil, J.F. (2003) *Geological Investigations Series* I-2781.

17. Delaney, M.L., Bé, A.W.H. & Boyle, E.A. (1985) *Geochimica et Cosmochimica Acta* **49,** 1327-1341.

18. Lea, D.W., Mashiotta, T.A. & Spero, H.J. (1999) *Geochimica et Cosmochimica Acta* **63,** 2369-2379.

19. Yang, C., Telmer, K. & Veizer, J. (1996) *Geochimica et Cosmochimica Acta* **60,** 851-866.

20. Mott, R.J., Grant, D.R., Stea, R. & Occhietti, S. (1986) *Nature* **323,** 247-250.

21. Swarzenski, P.W., Porcelli, D., Anderson, P.S. & Smoak, J.M. (2003) in *Uranium-Series Geochemistry: Reviews in Mineralogy & Geochemistry, 52,* eds Bourdon, B., Henderson, G.M., Lundstrom, C.C., Turner, S.P. (Mineralogical Society of America) pp. 577-606.

22. Russell, A.D. Emerson, S.R., Nelson, B.K., Erez, J., & Lea D.W. (1994) *Geochimica et Cosmochimica Acta* **58,** 671-681.

23. Chabaux, F., Riotte, J., Dequincey, O. (2003) in *Uranium-Series Geochemistry: Reviews in Mineralogy & Geochemistry, 52,* eds Bourdon, B., Henderson, G.M., Lundstrom, C.C., Turner, S.P. (Mineralogical Society of America) pp. 533-576.

24. Russell, A.D., Hönish, B., Spero, H.J. & Lea, D.W. (2004) *Geochimica et Cosmochimica Acta* **68,** 4347-4361.

25. Blum, J.D. & Erel, Y. (1997) *Geochimica et Cosmochimica Acta* **61**, 3193-3204.

26. Dyke, A. S. (2004) in *Quaternary Glaciations-Extant and Chronology*, eds Ehlers, J. Gibbard, P.L. (Elsevier Science and Technology Books, Amsterdam) Part II, vol. 2b, pp. 373-424.

27. Wadleigh, M.A., Veizer, J. & Brooks, C. (1985) *Geochimica et Cosmochimica Acta* **49,** 1727-1736.

28. Hostetler, S.W., Bartlein, P.J., Clark, P.U., Small, E.E. & Solomon, A.M. (2000) *Nature* **405**, 334-337.

29. Remenda, V.H., Cherry, J.A. & Edwards, T.W.D. (1994) *Science* **266,** 1975-1978.

30. Hillaire-Marcel, C. & Bilodeau, G. (2000) *Can. J. Earth Sci.* **37,** 795-809.

31. Flower, B.P., Hastings, D.W., Hill, H.W. & Quinn, T.M. (2004) *Geology* **32,** 597-600.

32. Smith, D.G. & Fisher, T.G. (1993) *Geology,* **21,** 9-12.

33. Teller, J.M. & Boyd, M. (2006) *Quaternary Science Reviews* **25,** 1142-1145.

34. Andrews, J.T. & Dunhill, G. (2004) *Quaternary Research* **61,** 14-21.

35. Manabe, S. & Stouffer, R.J. (1997) *Paleoceanography* **12,** 321-336.

36. DeMenocal, P., Ortiz, J., Guilderson, T. & Sarnthein, M. (2000) *Science* **288,** 2198-2202.

37. Lea, D.W., Pak, D.K., Peterson, L.C. & Hughen, K.A. (2003) *Science* **301,** 1361-1364.

38. Grootes, P.M., Stuiver, M., White, J.W.C., Johnsen, S. & Jouzel, J. (1993) *Nature* **369,** 552-554.

39. Genty, D. Blamart, D., Ghaleb, B., Plagnes, V., Causse, Ch., Bakalowicz, M., Zouari, K., Chkir, N., Hellstrom, J., Wainer, K. *et al.* (2006) Q*uaternary Science Reviews* **25**, 2118-2142.

40. Grafenstein, V. U., Erlenkeuser, H., Brauer, A., Jouzel, J. & Johnsen, J. (1999) *Science* **284**, 1654-1657.

41. Wang, Y.J. Cheng, H., Edwards, R.L., An, Z.S., Wu, J.Y., Shen, C.-C. & Dorale, J.A. (2001) *Science* **294,** 2345-2348.

42. Blunier, T. & Brook, E.J. (2001) *Science* **291**, 109-112.

43. Haley, B.A. & Klinkhammer, G.P. (2002) *Chemical Geology* **185,** 51-69.

44. Stuiver, M. Reimer, P.J., Bard, E., Beck J.W., Burr, G.S., Hughen, K.A., Kromer, B., McCormac, G., van der Plicht, J. & Spurk, M. (1998) *Radiocarbon* **40,** 1041-1083.

Figure 1. Bedrock map of central-eastern North America (16) showing major lithologies that influence river geochemistry. Colors are coded according to bedrock age: red shades are Precambrian, blue shades are Paleozoic, green shades are Mesozoic, and yellow is Cenozoic. We have identified those geochemical properties of bedrock types that produce distinctive signals in drainage basins. The western part of the Canadian Precambrian Shield has higher $^{87}Sr/^{86}Sr$ than the eastern Shield, Paleozoic sedimentary bedrock underlying the eastern Great Lakes includes Mg-rich dolomite, and Mesozoic sedimentary bedrock of the western Canadian Plains is enriched in U and Mg. Also shown is the outline (in blue) of the 12.5 cal. kyr BP ice margin (26), the southwestern margin of the Laurentide Ice Sheet at the start of the Younger Dryas (13 cal. kyr BP) and near the end of the Younger Dryas (11.5 cal. kyr BP) (26) (dashed black lines) (the age of these margins, however, is not constrained by dates (26)). The solid white line is the pre-Younger Dryas drainage area of the St. Lawrence River with its northern margin controlled by the ice sheet divide (7). The dashed white line represents the additional area routed to the St. Lawrence River at the start of the Younger Dryas (7). White arrows indicate the freshwater drainage routes to the Arctic, Gulf of Mexico and St. Lawrence River, and blue arrow indicates general location of eastern outlet for glacial Lake Agassiz. Core locations in outer St. Lawrence estuary are shown as red dot (core 90031-047) and yellow dot (core 90031-044).

Figure 2. Geochemical time series (in calibrated radiocarbon kyr BP) for the Younger Dryas interval. (a) Dinoflagellate cyst sea surface temperature reconstruction (HU90031-044) (9). (b) Planktonic (*N. pachyderma (s)*) $\delta^{18}O$ (gray) (11) and of seawater (blue) for the St. Lawrence (SL) (HU90031-044); and planktonic (*G. ruber*) $\delta^{18}O_{seawater}$ record from the Gulf of Mexico (GOM)

(purple) (31). Black squares denote the reported calibrated age control (31). (c) Planktonic (*N. pachyderma (s)*) $\delta^{13}C$ record (green) from the St. Lawrence (HU90031-044) (courtesy of C. Hillaire-Marcel). (d) Mg/Ca (gray) and ΔMg/Ca (black) of *G. bulloides* (HU90031-044). (e) U/Ca of *G. bulloides* (blue from HU90031-044, green from HU90031-047) and *N. pachyderma (s)* (red from HU90031-047). The offset in U/Ca between 044 and 047 prior to the Younger Dryas reflects the different proximity of the cores to the riverine end-member. (f) Sr-isotopes of *G. bulloides* (HU90031-044). White symbols with red outline represent TIMS measurements; red symbols with white outline represent multi-collector ICP-MS measurements. Gray bar denotes the time of eastward routing as inferred from our geochemical proxies of routing. Horizontal bars at bottom of graph indicate calibrated radiocarbon age control for core HU90031-044.

Figure 3. Time series (in calibrated radiocarbon kyr BP) of modeled freshwater discharge from the St. Lawrence River. The model is initiated with a flux of 0.07 Sv (7) and then solved to match the routing data (see supporting online methods). $^{87}Sr/^{86}Sr$ is in red, U/Ca in blue, $\delta^{18}O_{seawater}$ in black and ΔMg/Ca in purple with the gray bar denoting the ~30% propagated error (see supporting online methods).

Figure 4. Proxies of Atlantic meridional overturning circulation and freshwater routing. (a) $^{231}Pa/^{230}Th$ record from the subtropical North Atlantic (red diamonds are the ^{232}Th method, green diamonds are the ^{238}U method) (2). Age control indicated by black square. (b) Detrended $\Delta^{14}C$ from Cariaco Basin (1). (c) Planktonic U/Ca (blue), $\delta^{13}C$ (green) and $^{87}Sr/^{86}Sr$ (red) from HU90031-044. Vertical light gray bar denotes the timing of the Younger Dryas as inferred from

our geochemical proxies of routing and vertical dark gray bar denotes the intra-Younger Dryas event defined by our geochemical routing proxies.

Figure 5. Proxies of climate change and freshwater routing during the Younger Dryas. (a) Greenland $\delta^{18}O$ record (38). (b) $\delta^{18}O$ from Ammerssee Lake, Germany (40). (c) $\delta^{18}O$ from Chauvet Cave, France (39). Black symbols with error bars denote age control. (d) Sea surface temperature reconstruction from the coast of West Africa (36). Horizontal bars denote calibrated radiocarbon age control. (e) Planktonic U/Ca (blue), $\delta^{13}C$ (green), and $^{87}Sr/^{86}Sr$ from HU90031-044. (f) Sea surface temperature reconstruction from Cariaco Basin (37). (g) $\delta^{18}O$ from Hulu Cave, China (41). Black symbols with error bars denote age control. (h) $\delta^{18}O$ record from Byrd ice core, Antarctic (42). Vertical gray bars are the same as in Figure 4.

Table 1. Radiocarbon ages obtained from cores 047 and 044, including new ages from this study and previously published radiocarbon ages from core 044 (11). Calibrated ages are reservoir corrected (11, 26) and calibrated (44) with 1 sigma error.

Core	Depth (cm)	Material	Sample ID	^{14}C Age*	Calibrated Age Range
90031-044	20.3	N. pachyderma (s)	TO-4004	2610 ± 70	2150-2320
90031-044	40	N. pachyderma (s)	TO-4005	4230 ± 70	4150-4300
90031-044	140	N. pachyderma (s)	TO-4006	10040 ± 200	10570-10880
90031-044	180	N. pachyderma (s)	TO-4007	10500 ± 170	11290-11750
90031-044	220	N. pachyderma (s)	TO-4008	10840 ± 90	11940-12370
90031-044[a]	267	Shell	AA-57317	11520 ± 150	12870-13170
90031-044	300	N. pachyderma (s)	TO-4409	11890 ± 100	13150-13420
90031-044	410	N. pachyderma (s)	TO-4606	12890 ± 190	14700-15218
90031-044	550	N. pachyderma (s)	TO-4607	12950 ± 110	14740-15250
90031-047[a†]	426	Shell	CAMS-102060	11020 ± 120	12510-12750
90031-047[a]	444	Shell	CAMS-102059	10810 ± 45	12170-12490
90031-047[a]	496	Shell	CAMS-102061	11520 ± 310	12300-13850

*Not reservoir corrected

[a]New dates from this study

[†]Date excluded from the age model

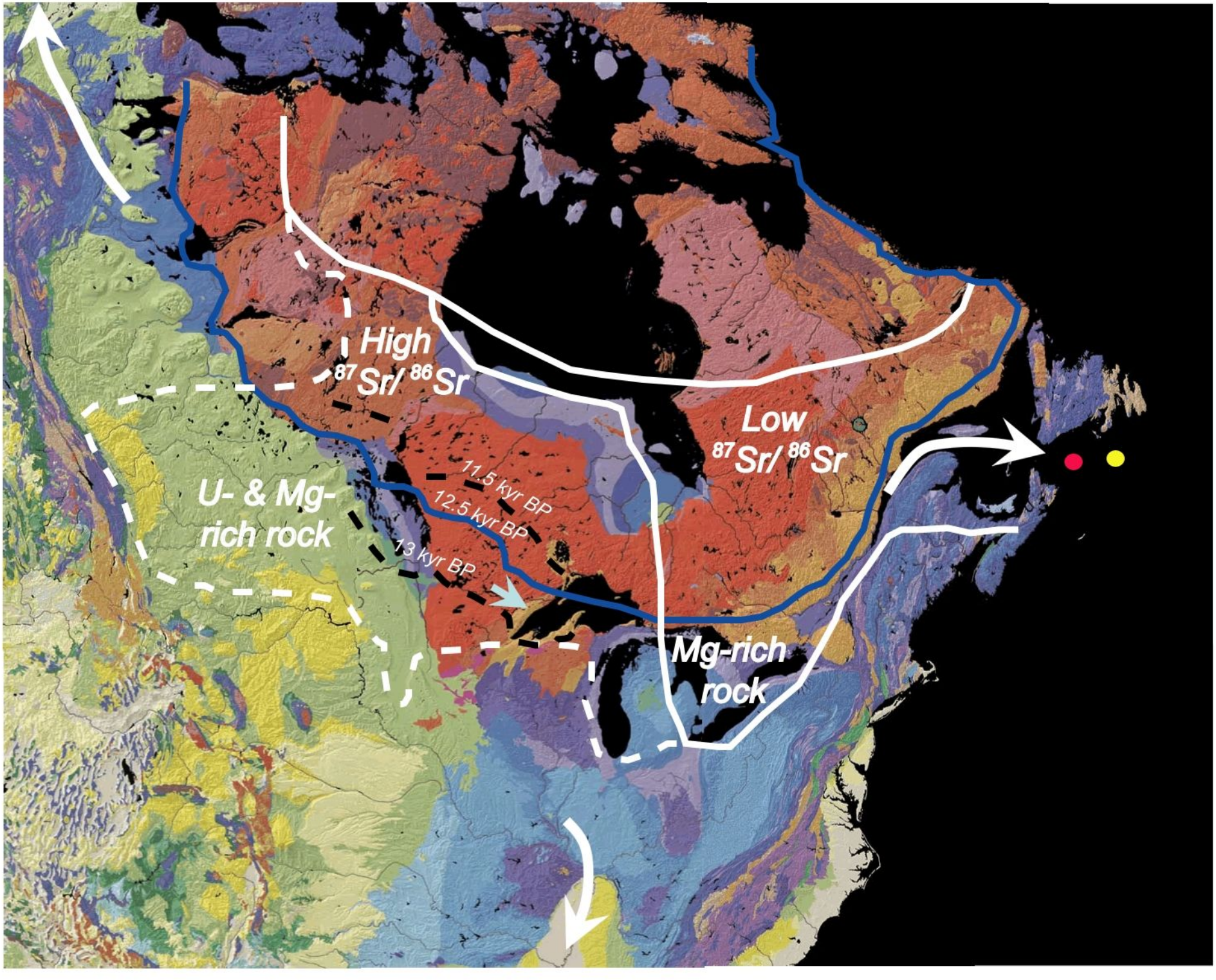
High
87Sr/86Sr
Low
87Sr/86Sr
U- & Mg-
rich rock
11.5 kyr BP
12.5 kyr BP
13 kyr BP
Mg-rich
rock

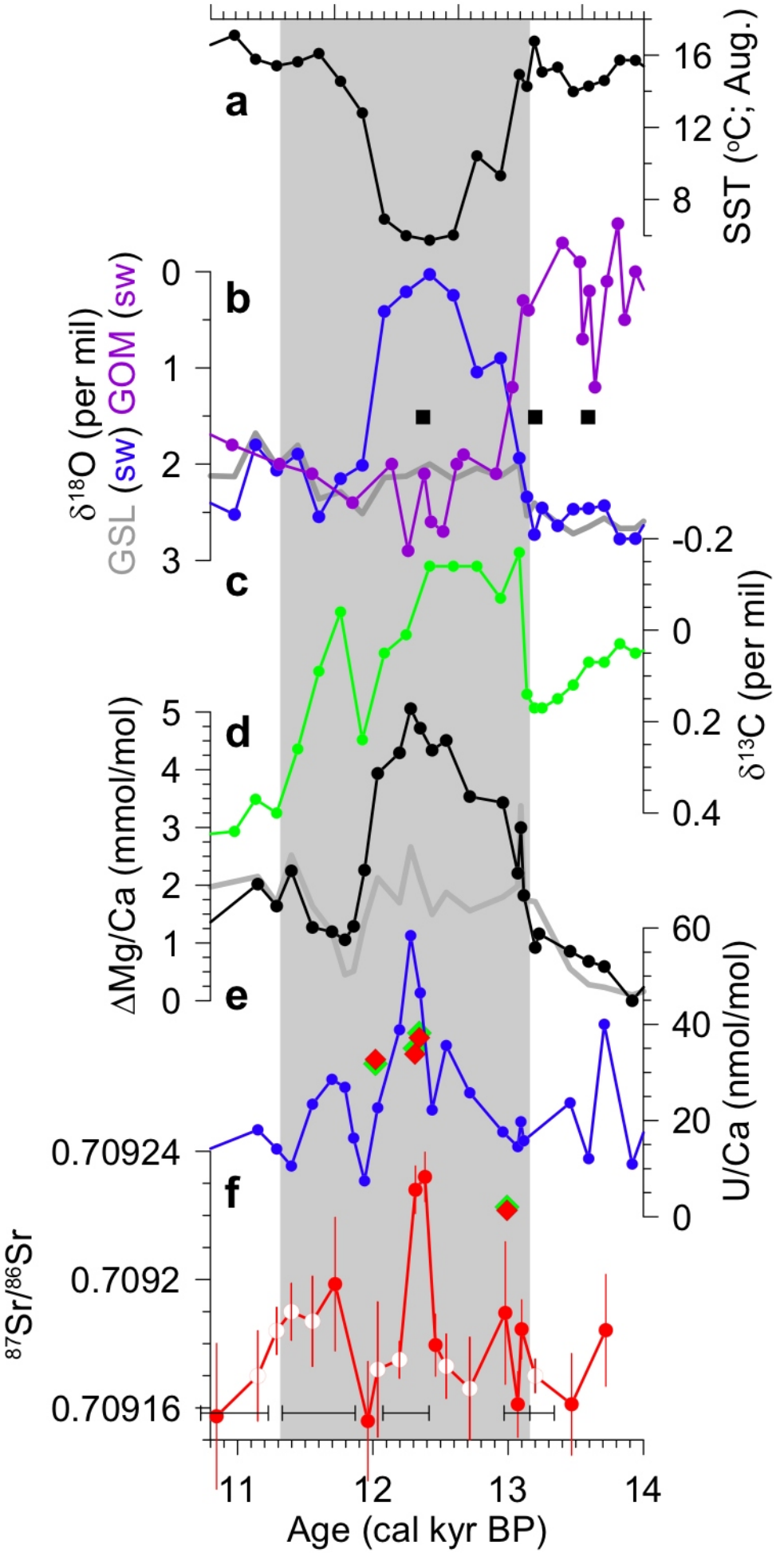
a
b
c
d
e
f
SST (°C; Aug.)
16
12
8
δ18O (per mil)
GSL (sw) GOM (sw)
0
1
2
3
δ13C (per mil)
-0.2
0
0.2
0.4
ΔMg/Ca (mmol/mol)
5
4
3
2
1
0
U/Ca (nmol/mol)
60
40
20
0
87Sr/86Sr
0.70924
0.7092
0.70916
11
12
13
14
Age (cal kyr BP)

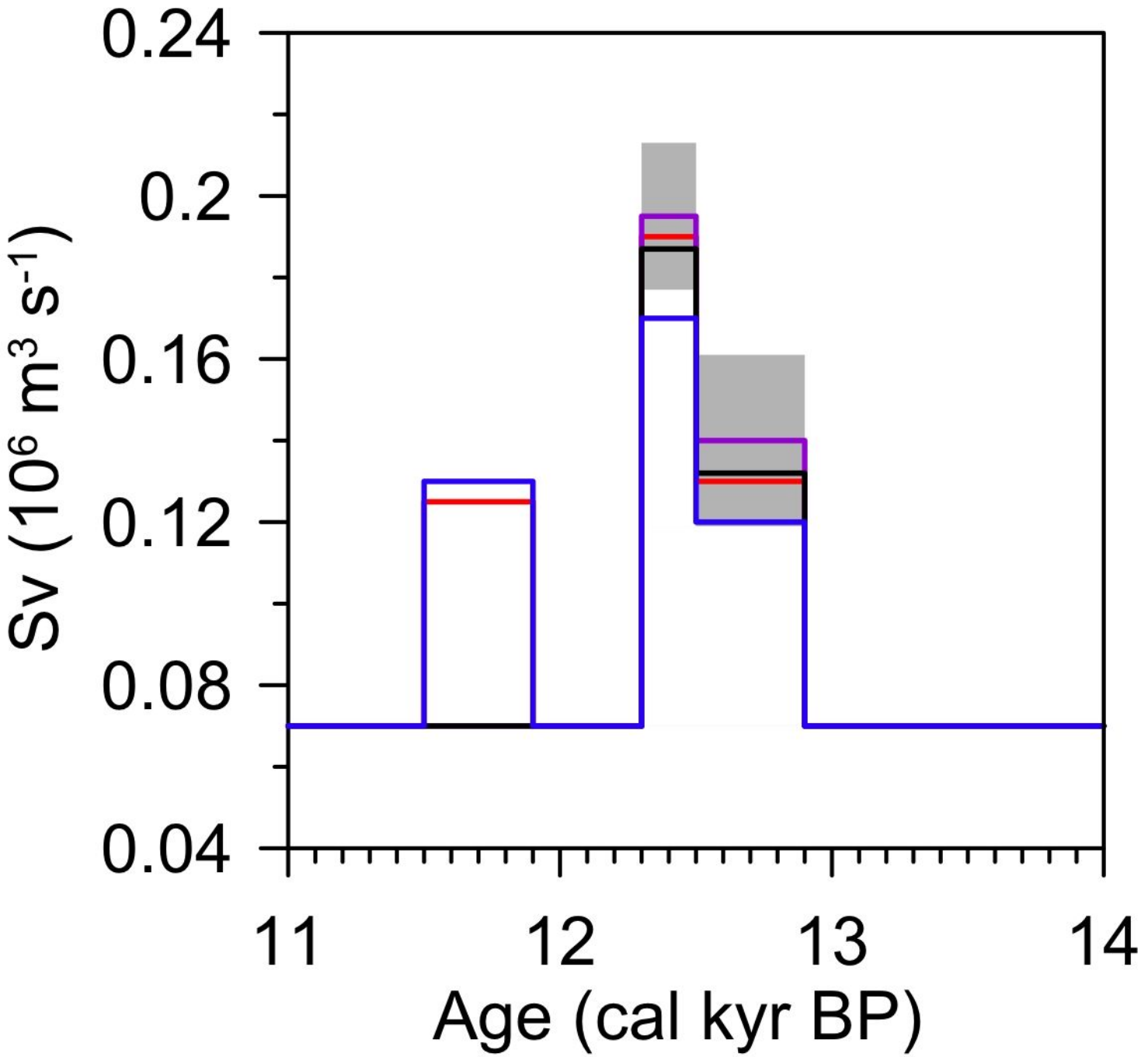
0.24
0.2
0.16
0.12
0.08
0.04
Sv (10⁶ m³ s⁻¹)
11
12
13
14
Age (cal kyr BP)

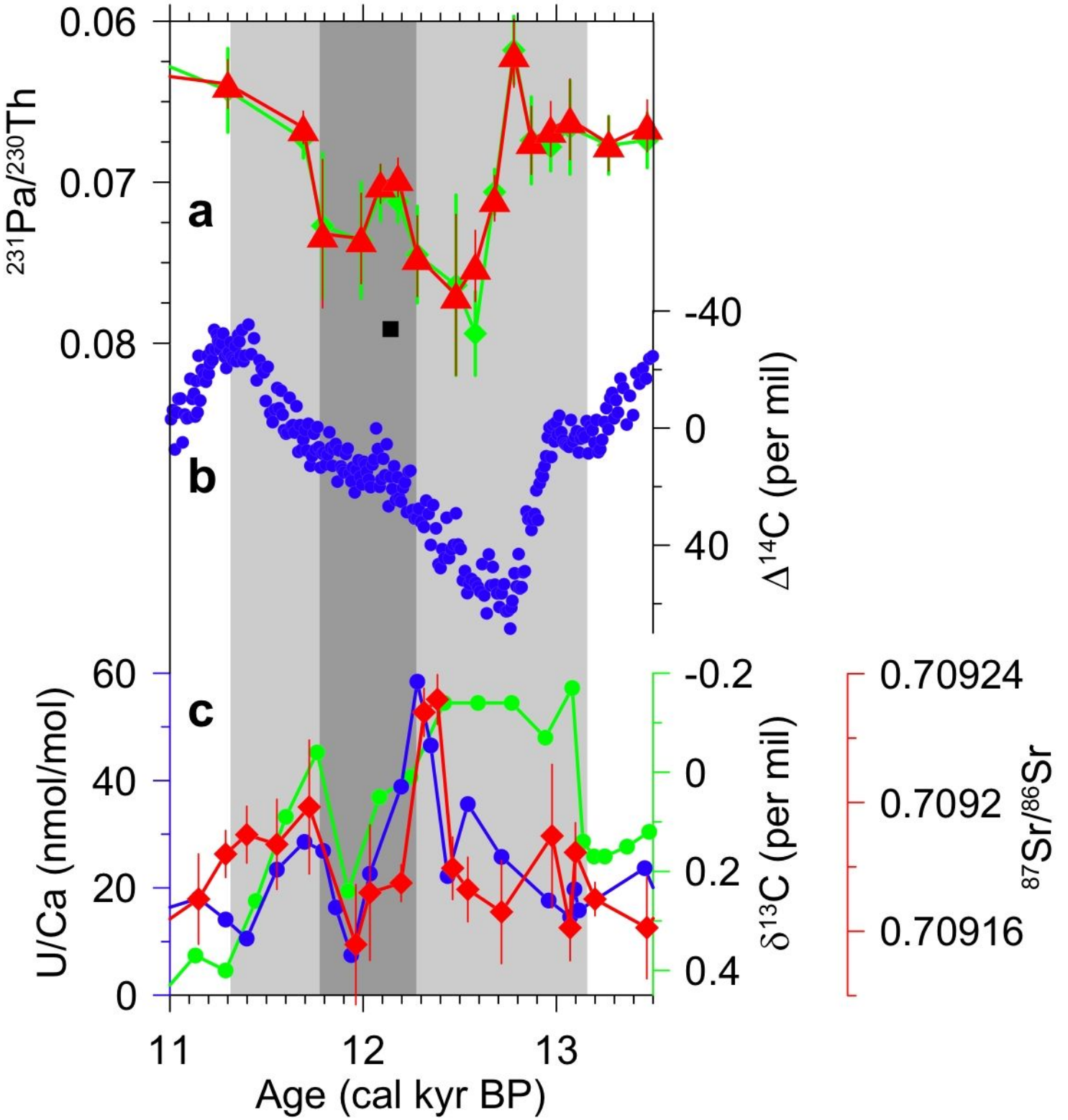
0.06
0.07
0.08
^{231}Pa/^{230}Th
a
b
c
-40
0
40
Δ^{14}C (per mil)
60
40
20
0
U/Ca (nmol/mol)
-0.2
0
0.2
0.4
δ^{13}C (per mil)
0.70924
0.7092
0.70916
^{87}Sr/^{86}Sr
11
12
13
Age (cal kyr BP)

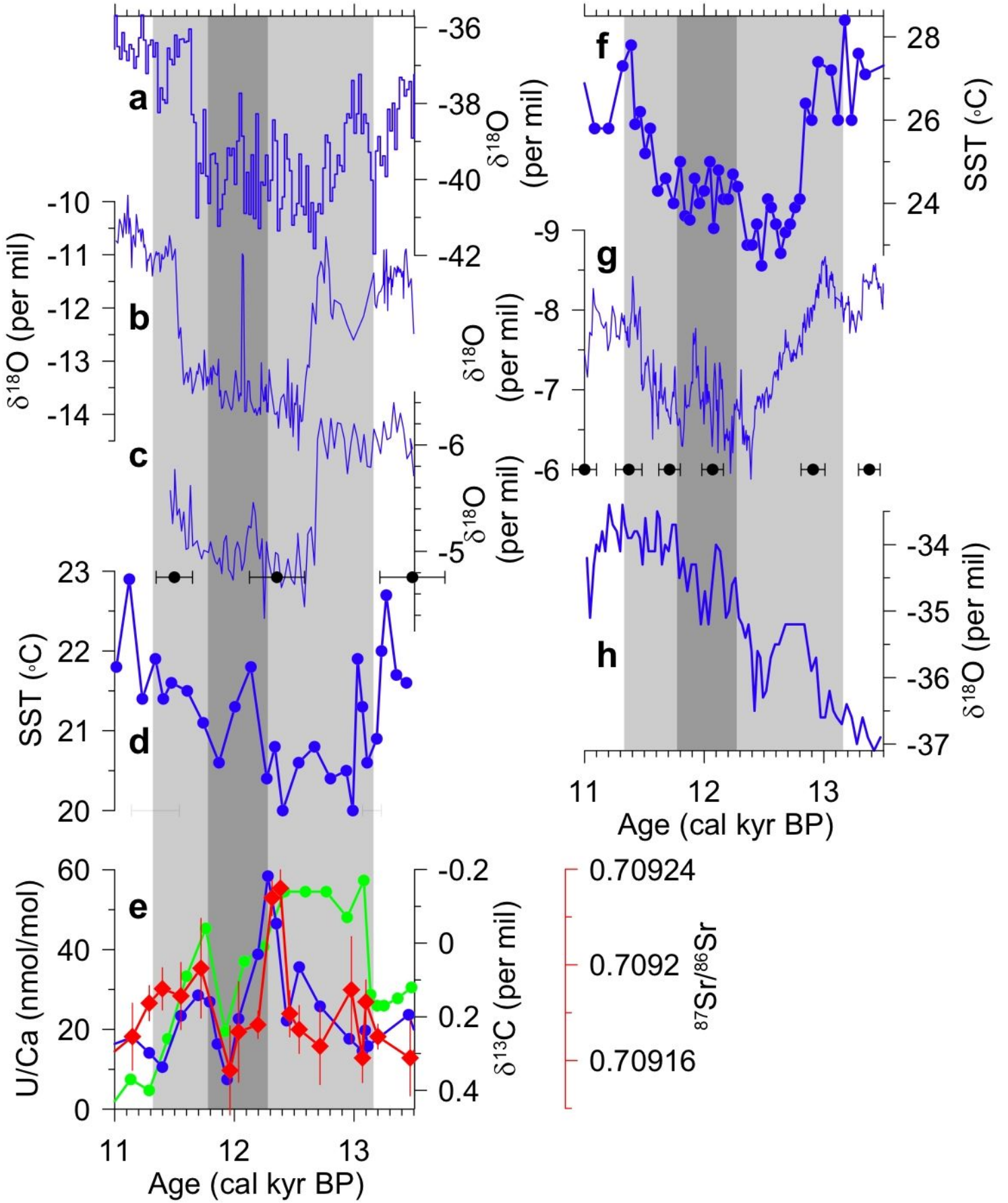
a
b
c
d
e
f
g
h
δ18O (per mil)
SST (°C)
U/Ca (nmol/mol)
δ13C (per mil)
87Sr/86Sr
Age (cal kyr BP)
11
12
13
-36
-38
-40
-42
-10
-11
-12
-13
-14
-6
-5
23
22
21
20
60
40
20
0
-0.2
0
0.2
0.4
0.70924
0.7092
0.70916
28
26
24
-9
-8
-7
-6
-34
-35
-36
-37

SUPPORTING ONLINE METHODS

Error Propagation. The error involved in the relationship between salinity and $\delta^{18}O_{seawater}$ is at most ~20% (with $\delta^{18}O_{seawater}$ having a sensitivity of 35% to changes in salinity) (1, 2), the error in the Mg/Ca:sea surface temperature (SST) relationship is less than 10% (with Mg/Ca having a 10% sensitivity to changes in SST) (3-5), the error in Mg/Ca:salinity relationship is ~75% (with Mg/Ca having a 4% sensitivity to changes in salinity) (3) and the error in the dynoflagellate SST reconstruction is 18 to 20% (6). We use the equation for error propagation (7):

$$\sigma_x^2 = \sigma_u^2\left(\frac{\partial x}{\partial u}\right)^2 + \sigma_v^2\left(\frac{\partial x}{\partial v}\right)^2 + \ldots$$

where σ_x is the propagated error of a given proxy, x; σ_u and σ_v and so on are the errors of other proxy reconstructions (u, v, etc.) influences' on x weighted by the square of the sensitivity of x to these changes (the partial derivative $\frac{\partial x}{\partial u}$ and $\frac{\partial x}{\partial v}$ and so on). We apply this to our data as (in general form):

σ_x = ((salinity: $\delta^{18}O_{seawater})_{global}$ + $(Mg/Ca:SST)_{global}$ + $(Mg/Ca:salinity)_{global}$ + (SST: $\delta^{18}O_{seawater})_{local}$ + $(SST:Mg/Ca)_{local}$

where subscript "global" refers to general relation and subscript "local" refers to that specific to the St. Lawrence SST reconstruction. Thus:

$\sigma_x = (0.2^2*0.35^2+0.1^2*0.1^2+0.75^2*0.04^2+0.2^2*0.35^2+0.2^2*0.1^2)^{-2}=0.106$

And:

0.106+0.20 (the original error) = 0.306 or ~30% error.

Geochemical Mixing Models. We model changes in estuary geochemistry based on foraminifera $\delta^{18}O_{seawater}$ and [U], [Ca] and [Mg] using a simple flux-weighted mixing model. The model has five components: the isotopic ratio or concentration (mol/kg) of the ocean end-member (I_o), the flux of the ocean water to the estuary (F_o, Sv), the isotopic ratio or concentration (mol/kg) of the river end-member (I_r), the river flux (F_r, Sv), and the estuary isotopic ratio or concentration (mol/kg) (I_e):

$$I_e = \frac{F_r I_r + F_o I_o}{F_r + F_o}.$$

In the case of Sr-isotopes, we must also consider changes in the river [Sr] (Y_r, mol/kg) and changes in the isotopic ratio (T_r) as well as the concentration (Y_o, mol kg^{-1}) and isotopic ratio (T_o) of the ocean:

$$I_e = \frac{Y_r F_r T_r + Y_o F_o T_o}{Y_r F_r + Y_o F_o}.$$

I_o, Y_o and F_o are considered constants. I_o and Y_o are calculated from the conservative behavior of U, Mg, Ca and Sr in the ocean. F_o comes from the net flux of ocean water into the St. Lawrence below 100 m depth (~0.74 Sv) (8). We assume that all of this water exits in the upper 100 m mixed layer, corresponding to the habitat of *G. bulloides* and *N. pachyderma (s)* (6). This discharge depends on the bathymetry of the St. Lawrence estuary. To account for any changes in bathymetry, we correct for sea level lowering and isostatic depression as well as the marine incursion of the Champlain Sea (9). These corrections, however, do not substantially change the geometry of the estuary from its modern shape. Also, our core locations are at the river distal end of the estuary and the chemistry there would likely not be influenced by a shift in the river-ocean mixing front due to an increase in river flux.

For Sr- and O-isotopes, we use previously determined ratios and concentrations for T_r and I_r. We use the modern Sr-isotope ratio for T_r (10) and the modern ocean ratio of 0.70917 for T_o. For modeling the Sr-isotope spike at ~12.5 kyr BP due in part to the retreat of the southwestern margin of the Laurentide Ice Sheet exposing fresh shield bedrock, we use the Sr-isotope value of 0.79500 from Blum & Erel (11) determined on Precambrian bedrock that was exposed for 400 years. For O-isotopes, we use a $\delta^{18}O$ of -25 per mil for Lake Agassiz freshwater (I_r) (12) and $\delta^{18}O$ of 0 per mil for I_o.

To determine the river [U], [Mg], [Ca] (I_r) and [Sr] (Y_r), we model basin-scale river geochemistry using a combination of previously measured modern river concentrations on known rock types (10, 13-15) and river geochemistry data supplied by the Saskatchewan Watershed Authority. These concentrations are weighted by the exposure area of a given rock type relative to the basin area to determine the element concentration (X, mol/kg) of river water leaving the basin:

$$X = \sum_{i}^{n} \frac{A_i}{A_b} R_i$$

where A_i (m^2) is the exposed area of a specific rock type, A_b (m^2) is the area of the cryohydrological basins defined by Licciardi et al. (16), and R_i (mol/kg) is the element river-water concentration for a given rock type. These basin concentrations are then weighted by their discharge and summed to calculate the [U], [Mg], [Ca] (I_r) and [Sr] (Y_r) in water discharged to the ocean through a given outlet:

$$I_r(Y_r) = \sum_{j}^{n} X_j W$$

where W is a constant of proportionality that weights the chemistry of a basin by the discharge of the basin relative to the total discharge through an outlet (F_r). We initialize

our value of W according to the discharges for each basin derived by Licciardi *et al.* (16). We then assume that any change in total discharge through an outlet as needed to match our data will be accompanied by a proportional change in discharge from each basin so that W remains constant. These model results in the river end member concentrations listed in supporting online Table 2.

To calculate discharge from our data, we convert modeled [U], [Mg] and [Ca] into estuary foraminiferal U/Ca and ΔMg/Ca records following Russell *et al.* (17) and Delaney *et al.* (18), respectively, which can then be compared against our data. We initialize our model with the river discharge (F_r = 0.07 Sv) of Licciardi *et al.* (16) prior to the Younger Dryas. We then solve our model for discharge (F_r) at the initial increase at the start of the Younger Dryas, the peak discharge during the Younger Dryas, the intra-Younger Dryas event, and the subsequent rerouting event near the end of the Younger Dryas. We determine the error in our discharge estimates using two standard deviations in discharge between the independent routing proxies from the average of all the proxies.

In using modern river data, we assume that chemical weathering rates during the Younger Dryas were analogous to modern weathering rates, which introduces some unknown error into our calculations. The error that we calculate for our base discharge estimate, however, likely encompasses any climate-induced changes in the weathering. In addition, the surface of the western Canadian Plains is covered by glacial till with a composition of primarily locally derived bedrock and Canadian Shield, creating a homogeneous weathering source for our freshwater tracers. The residence time of freshwater in Lake Agassiz may also have affected water chemistry. However, with a volume of 1,400 km^3 after the initial lake drainage (19), the residence time of water in

Lake Agassiz is 160 ± 40 days, which is likely of short enough duration that limnologic processes had little effect on water chemistry.

Additionally, this model does not account for any consumption or production of Mg, Sr, Ca or U in the estuary. It is well established that Mg, Sr and Ca behave conservatively in estuarine environments. In contrast, U can be consumed by particulate rain at low salinities (practical salinity units (psu) <10) and produced by colloid and particulate disintegration at high salinities (psu. >20) (20). The actual contribution of these processes is variable for different river systems. However, given the exponential relation between suspended load and discharge, we attempt to include the effect of U release from colloids and particulate matter at high salinities in the mixing model by:

$$Z = 0.579 \exp(7.66 F_r)$$

where Z is the percentage of the U released from particulate/colloid break down relative to the [U] in solution. The relation was determined assuming a maximum U contribution from colloids and particulates of 245% for a discharge of 0.20 Sv (20). There is an unknown amount of error in this calculation, but the calculations do cover the known range of U sourced from colloidal and particulate break-down (20).

$\delta^{18}O$ and % *N. pachyderma (s.)* records from continental margin off Nova Scotia. We reproduce the stacked $\delta^{18}O_{calcite}$ record measured on *N. pachyderma* (21) (supporting online Fig. 6a), which shows a Younger Dryas signal of ~0.8 per mil. Subtracting the secular change in $\delta^{18}O_{seawater}$ associated with global sea level rise of the last deglaciation (22) from this record emphasizes the Younger Dryas signal (supporting online Fig. 6b). The record of % *N. pachyderma (s.)* from the same cores (supporting online Fig. 6c)

suggests that substantial Younger Dryas cooling occurred, which, if accounted for, would further increase the $\delta^{18}O$ signal.

Supporting Online Methods References

1. Fairbanks, R.G., Evans, M.N., Rubenstone, J.L., Mortlock, R.A., Broad, K., Moore, M.D. & Charles, C.D. (1997) *Coral Reefs* **16,** 93-100.
2. Morimoto, M., Abe, O., Kayanne, H., Kurita, N., Matsumoto, E. & Yoshida, N. (2002) *Geophys. Res. Lett.* **29,** 10.1029/2001GL013521.
3. Lea, D.W., Mashiotta, T.A. & Spero, H.J. (1999) *Geochimica et Cosmochimica Acta* **63,** 2369-2379.
4. Mashiotta, T.A., Lea, D.W. & Spero, H.J. (1999) *Earth and Planetary Science Letters* **170,** 417-732.
5. Elderfield, H. & Ganssen, G. (2000) *Nature* **405,** 442-445.
6. deVernal, A., Hillaire-Marcel, C. & Bilodeau, G. (1996) *Nature* **381,** 774-777.
7. Bevington, P. & Robinson, D. K. (2003) *Data Reduction and Error Analysis for the Physical Sciences* (McGraw Hill, Columbus, OH) pp. 41.
8. Dickie, L.M. & Trites, R.W. (1983) in *Ecosystems of the World 26, Estuaries and Enclosed Seas*, ed Ketchum, B.W. (Elsevier Scientific Publishing Company, New York) pp. 403-425.
9. Shaw, J., Gereau, P. & Courtney, R.C. (2002) *Quaternary Science Reviews* **21,** 1861-1878.
10. Wadleigh, M.A., Veizer, J. & Brooks, C. (1985) *Geochimica et Cosmochimica Acta* **49,** 1727-1736.
11. Blum, J.D. & Erel, Y. (1997) *Geochimica et Cosmochimica Acta* **61**, 3193-3204.
12. Remenda, V.H., Cherry, J.A. & Edwards, T.W.D. (1994) *Science* **266,** 1975-1978.

13. Meybeck, M. (1987) *American Journal of Science* **287,** 401-428.

14. Yang, C., Telmer, K. & Veizer, J. (1996) *Geochimica et Cosmochimica Acta* **60,** 851-866.

15. Chabaux, F., Riotte, J. & Dequincey, O. (2003) in *Uranium-Series Geochemistry: Reviews in Mineralogy & Geochemistry, 52,* eds Bourdon, B., Henderson, G.M., Lundstrom, C.C., Turner, S.P. (Mineralogical Society of America) pp. 533-576.

16. Licciardi, J.M., Teller, J.T. & Clark, P.U. (1999) in *Mechanisms of Global Climate Change at Millennial Time Scales: Geophysical Monograph* eds Clark, P.U., Webb, R.S., Keigwin, L.D. (AGU, Washington , D.C.) vol. 112*,* pp. 177-201.

17. Russell, A.D. Emerson, S.R., Nelson, B.K., Erez, J. & Lea D.W. (1994) *Geochimica et Cosmochimica Acta* **58,** 671-681.

18. Delaney, M.L., Bé, A.W.H. & Boyle, E.A. (1985) *Geochimica et Cosmochimica Acta* **49,** 1327-1341.

19. Leverington, D.W., Mann, J.D. & Teller, J.T. (2002) *Quaternary Research* **57,** 244-252.

20. Swarzenski, P.W., Porcelli, D., Anderson, P.S., & Smoak, J.M. (2003) in *Uranium-Series Geochemistry: Reviews in Mineralogy & Geochemistry, 52,* eds Bourdon, B., Henderson, G.M., Lundstrom, C.C., Turner, S.P. (Mineralogical Society of America) pp. 577-606.

Supporting Online Table 2. Element concentrations for the St. Lawrence River end member determined by bedrock type and area.

Element	Pre-Younger Dryas	Early Younger Dryas	Peak Younger Dryas
U (mol kg^{-1})	1.22×10^{-9}	1.01×10^{-8}	2.33×10^{-8}
Mg (mol kg^{-1})	1.00×10^{-4}	6.00×10^{-4}	9.8×10^{-4}
Ca (mol kg^{-1})	2.50×10^{-3}	1.10×10^{-3}	1.00×10^{-3}

Supporting Online Figure 6. (a) The stacked $\delta^{18}O_{calcite}$ record measured on *N. pachyderma (s)* from five cores from the continental margin of Nova Scotia (1) (solid line with symbols), and the secular change in $\delta^{18}O_{seawater}$ associated with global sea level rise of the last deglaciation (2) (solid gray line). (b) The stacked Nova Scotia margin $\delta^{18}O_{calcite}$ record after subtraction of the $\delta^{18}O_{seawater}$ record. (c) The record of % *N. pachyderma (s)* from core HU73031-7 (1). Radiocarbon age control for this core shown by squares. Keigwin and Jones (1) note that the 400-year reservoir age correction may be a minimum, given evidence from elsewhere in the North Atlantic for a larger reservoir age correction during the Younger Dryas (3).

Supporting Online Figure 6 References

1. Keigwin, L.D. & Jones, G.A. (1995) *Paleoceanography,* **10,** 973-985.

2. Fairbanks, R.G. (1989) *Nature* **342**, 637-642.

3. Bard, E. Arnold, M., Mangerud, J., Paterne, M., Labeyrie, L., Duprat, J., Mélières, M.-A., Sønstegaard, E., & Duplessy, J.-C. (1994) *Earth and Planetary Science Letters* **126**, 275-287.

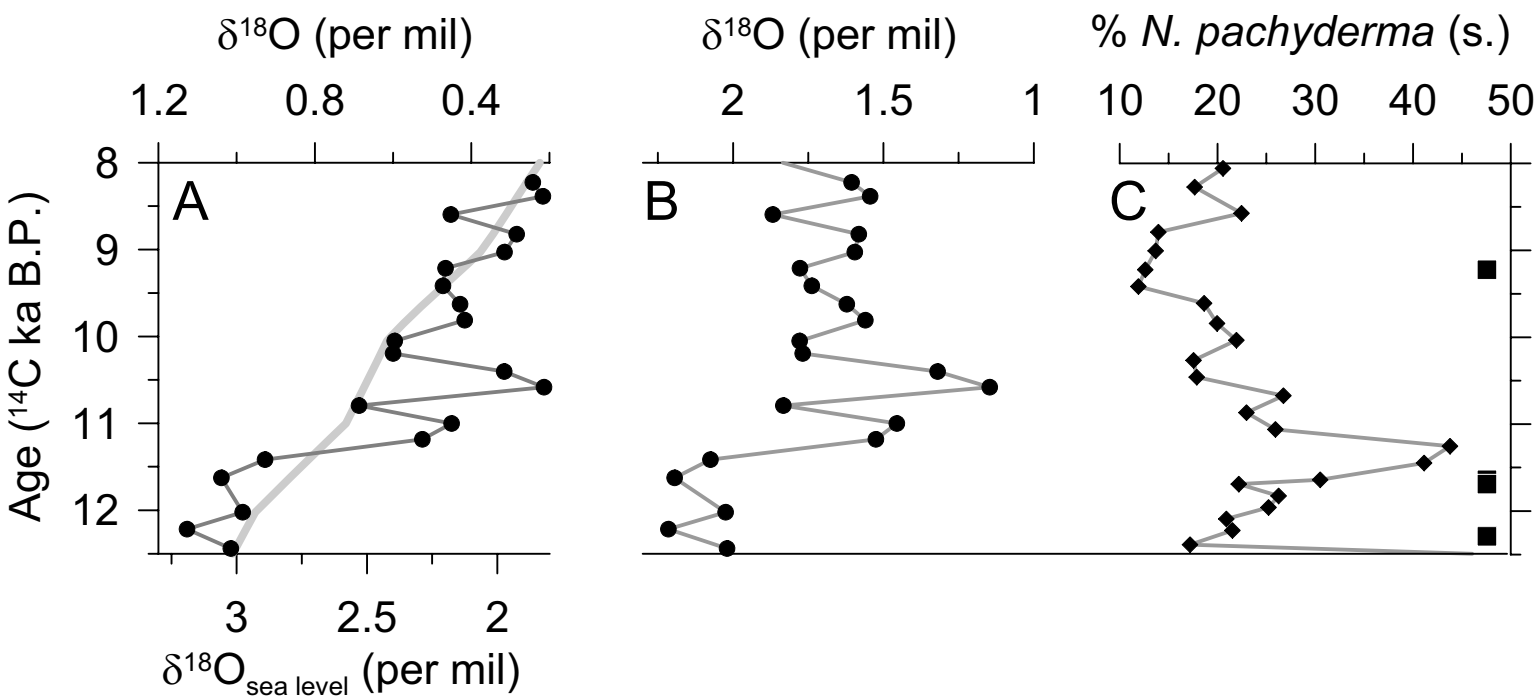
δ18O (per mil)
1.2
0.8
0.4
A
δ18O (per mil)
2
1.5
1
B
% N. pachyderma (s.)
10
20
30
40
50
C
Age (14C ka B.P.)
8
9
10
11
12
3
2.5
2
δ18Osea level (per mil)